J Solution Chem
DOI 10.1007/s10953-015-0373-6

Photo-Induced Intermolecular Electron Transfer from Donating Amines to Accepting Diarylethylenes in Different Solvents

Marwa N. El-Nahass[1] · Tarek A. Fayed[1] · Mohammed A. El-Morsi[1]

Received: 4 May 2013 / Accepted: 7 April 2015

Abstract The fluorescence quenching of newly synthesized diarylethylenes by some aliphatic and aromatic amines has been carried out at room temperature in solvents of various polarities and viscosities including acetonitrile, methanol, ethanol, and cyclohexane using steady-state measurements. Additionally, the cyclic voltammetric behavior of the investigated diarylethylenes has been studied, in order to determine their reduction potentials, which are necessary for calculation the Gibbs energy change for the photoinduced, electron transfer (ET) reactions in diarylethylene–amine systems. No change in the shape of the fluorescence spectra was observed, except for diarylethylenes–*N*,*N*-dimethyl aniline pairs in cyclohexane at which an exciplex was observed. The quenching mechanism is due to the ET from the ground state amines to the excited diarylethylenes. Both linear and non-linear Stern–Volmer behaviors have been encountered. The observed k_q values for different diarylethylenes–amine pairs do not correlate with the basicity (pK_b) of the amines but decrease with increasing the oxidation potentials of the amines. The bimolecular quenching rate constants have been correlated with ΔG° values for the ET reactions according to the Marcus outer-sphere ET theory.

Keywords Fluorescence quenching · Cyclic voltammetric behavior · Exciplex · Electron transfer · Aliphatic amines · Aromatic amines

1 Introduction

Diarylethenes with heterocyclic rings have been developed as novel classes of therapeutic compounds shown to exert a wide range of biological activities. Initially employed as pigments in leather tanning, most of the compounds that exhibited both high levels of

✉ Marwa N. El-Nahass
marwacu@yahoo.com; marwa.elnahas@science.tanta.edu.eg

[1] Chemistry Department, Faculty of Science, Tanta University, Tanta 31527, Egypt

Published online: 05 September 2015

fluorescent properties and a capacity to bind with cellular structures were extensively used as fluorochromes [1]. They have been investigated for their clinical efficacy as an ophthalmic drug, to lower intraocular pressure, and for anti-tumor and anti-HIV activities [2]. Also, they have been used as novel fluorescent substrates for the localization of peroxidase activity [3], antiproliferative agents [4], nonlinear optical materials [5] and emitter material in organic electroluminance devices [6].

Electron transfer (ET) reactions are one of the most interesting subjects and have experienced extensive experimental and theoretical studies in recent decades [7, 8]. Studies on ET reactions have importance from the view point of both academic and applied implications, as these reactions are important in chemistry and biology. Understanding of the various factors that control ET reactions is the main impetus in most of studies on ET processes. Photoinduced ET reactions where either the acceptor or the donor is photoexcited to trigger the reaction have been extensively studied to investigate various factors that control the mechanisms and dynamics of ET in various ET systems. In some of the earlier studies on bimolecular ET reactions [9–11], it was observed that the quenching process is largely dependent on the aliphatic and aromatic nature of the quenchers. The fluorescence quenching for a series of acceptors by different aliphatic and aromatic amines as electron donors have been investigated in acetonitrile solutions under diffusion conditions, aiming to understand how the nature of the amines affects the ET process. In addition to the noncyclic aliphatic amines, cyclic amines like 1-azabicyclo-[2]-octane (ABCO) and 1,4-diazabicyclo-[2]-octane (DABCO) have been also used to obtain better understanding and interpretation of the observed results [12]. Therefore, our work aimed at studying the cyclic voltammetric behavior of the newly synthesized diarylethylenes, in order to determine their reduction potentials, which are necessary for calculation the Gibbs energy change for the photoinduced, ET reactions in diarylethylene–amine systems. Also, the fluorescence quenching of the investigated diaryethylenes with some amines as electron donors has been studied using steady-state fluorescence spectroscopy, to give insights into the factors affecting the photoinduced ET reactions. Finally, the rationalization of the experimental data in terms of Marcus theory and Rehm–Weller model has been studied.

2 Experimental

The investigated 1-Ar-2-(2-benzothiazolyl) ethenes (Ar = phenyl, 1-naphthyl and 2-naphthyl) were synthesized by condensation of 2-methylbenzothiazole with the corresponding arylaldehyde [13], as follows: equimolar quantities of 2-methylbenzothiazole and the corresponding arylaldehyde were dissolved in an alkaline solution of dimethylformamide (containing 4 g KOH per 50 mL) then the solution was stirred for 3 h; after that, drops of 0.1 mol·dm^{-3} HCl were added to the pre-cooled reaction mixture reaction mixture until complete precipitation. The products were removed by filtration and purified by recrystalization twice from dry ethanol. The purity of the prepared compounds was checked by UV–Vis, fluorescence spectroscopy and melting point measurements. The compounds have a pale yellow color. Amine samples were *N*,*N*-diethylethanamine (TEA, Aldrich), *N*,*N*′-dimethylaniline (DMA, Fluka) and aniline which were purified by distillation under reduced pressure, while 1,4-diazabicyclo[2]octane (DABCO, Aldrich) was sublimed before use. Chemical structures of the diarylethylenes are shown in Scheme 1, along with their abbreviations. All solvents used were of spectroscopic grade (Aldrich or Merck) except ethanol and methanol, which were purified by double distillation before use.

Scheme 1 Structures and abbreviations of the prepared 1-Ar = 2-(2-benzothiazolyl) ethenes

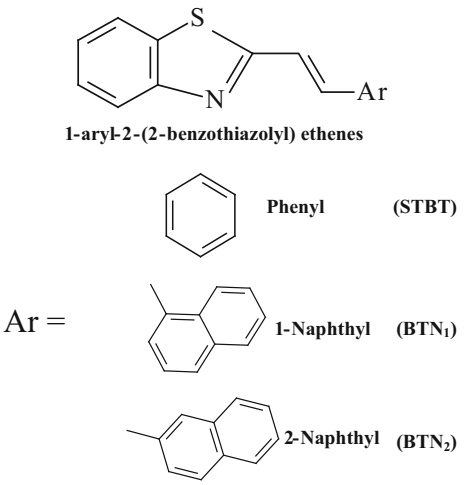

The reduction potentials were measured using cyclic voltammetry. Voltammetric measurements were carried out using an electrochemical (Pyrex) cell comprising three electrodes immersed in a solution containing the investigated compounds. One of the three electrodes is the working electrode, which was a hanging mercury drop (HDME, geometrical area 0.026 cm^2), the second electrode was the reference electrode (Ag/AgCl), and the third electrode was the counter electrode.

The absorption spectra were recorded on a Shimadzu UV–Vis 3101 PC spectrophotometer, while the emission spectra were measured using a Perkin-Elmer LS50B luminescence spectrometer using matched quartz cuvettes.

3 Results and Discussion

3.1 Cyclic Voltammetric Behavior of 1,2-Diarylethylene Derivatives in Universal Buffer Solutions

To determine the reduction potentials of the 1-Ar-2-(2-benzothiazolyl) ethenes (Ar = phenyl, STBT, 1-naphthyl, BTN_1 and 2-naphthyl, BTN_2), which are necessary for calculation of the Gibbs energy changes of the photoinduced ET reactions in the diarylethylenes–amine systems, the electrochemical reduction was studied in universal buffer solutions having pH values 4, 7 and 10 using sample concentrations of 1×10^{-3} mol·dm^{-3}, at room temperature. The recorded cyclic voltammograms show a single well defined cathodic peak, which was attributed to the reduction of the diarylethylenes. The reduction wave is in the potential range of −0.85 to −1.8 V versus the Ag^+/AgCl electrode throughout the pH range studied. At pH = 4, the peak of the reduction wave of BTN_1 is located at −0.98 V at a scan rate of 500 mV·s^{-1}, as an example. On increasing the pH of the solution, the peak potential (E_{pc}) is shifted to more negative values and the peak current (i_p) varied as well (Fig. 1). The larger shift in the E_{pc} values was found at pH = 10, indicating participation of hydrogen ions in the electrode process. The relation of E_{pc} to pH is shown in Fig. 2. Examination of the cyclic voltammograms obtained at different scan

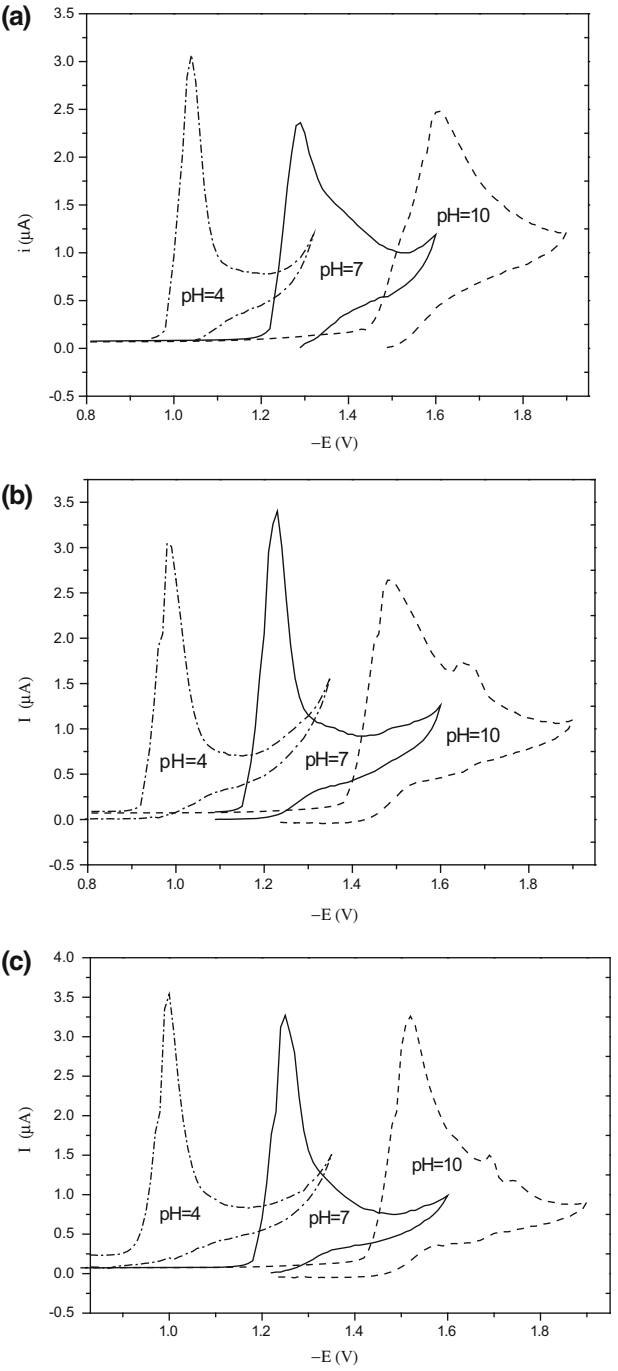

Fig. 1 Cyclic voltammograms of **a** STBT, **b** BTN_1, and **c** BTN_2 at scan rate 500 $mV{\cdot}s^{-1}$ in different buffer solutions

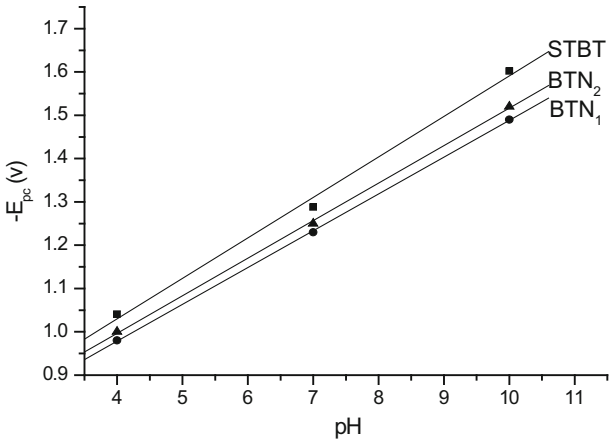

Fig. 2 The relation of E_{pc} versus pH for the investigated compounds at scan rate 500 mV·s^{-1}

rates within the range of 100–500 mV·s^{-1} at pH = 4 reveals that no anodic counter part is seen on the reverse sweep, indicating either the reduction is totally irreversible, which is unlikely, or the reduction product is consumed rapidly by another processes, e.g., protonation or dimerization. Also, the peak potential was shifted to more negative potentials on increasing the scan rate. A similar behavior is obtained at pHs 7 and 10. The typical voltammograms recorded at various potential scan rates for the compounds under investigation in different buffers are shown in Fig. 3. As shown from these figures, the peak potential (E_{pc}) and the peak current (i_{pc}) were strongly affected by changing the scan rate. The large decrease in the peak current indicates that the product formed is strongly adsorbed at the electrode surface.

Since the peak potential, the peak current and the current function ($i_{pc}/v^{1/2}$) depend on the scan rate, the variations of the cathodic peak potential and peak current with the scan rate were analyzed by plotting i_{pc} against the square root of scan rate ($v^{1/2}$). Linear dependences were obtained as is shown in Fig. 4. These results confirm the previous conclusion regarding the irreversibility of the process. This linear dependence indicates that the reduction process is diffusion-controlled [14]. Also, the dependence of the current function ($i_{pc}/v^{1/2}$) on $v^{1/2}$ is shown in Fig. 5. The dependence of $i_{pc}/v^{1/2}$ on $v^{1/2}$ is an important diagnostic criterion for establishing the type of mechanism by cyclic voltammetry. Tables 1, 2, and 3, show the electrochemical data for the reduction of these compounds at different pH values and the different values of $i_{pc}/v^{1/2}$ for the investigated compounds as a function of scan rate. From the data reported in these tables, it was found that the value of $i_{pc}/v^{1/2}$ decreases as the scan rate increases. From these results it was concluded that the compounds are reduced electrochemically in a diffusion controlled irreversible process.

3.2 Steady-State Fluorescence Quenching Studies

With the aim of collecting information about the excitation and emission maxima, which are necessary for quenching measurements, ground state absorption spectra and steady state fluorescence spectra of the investigated diarylethylenes were recorded in different solvents of various polarities and viscosities including acetonitrile (ACN), methanol (MeOH), ethanol (EtOH), and cyclohexane. All measurements were carried out in the dark to avoid any photochemical reactions. Table 4 lists the absorption maxima (λ^{A}_{max}) and

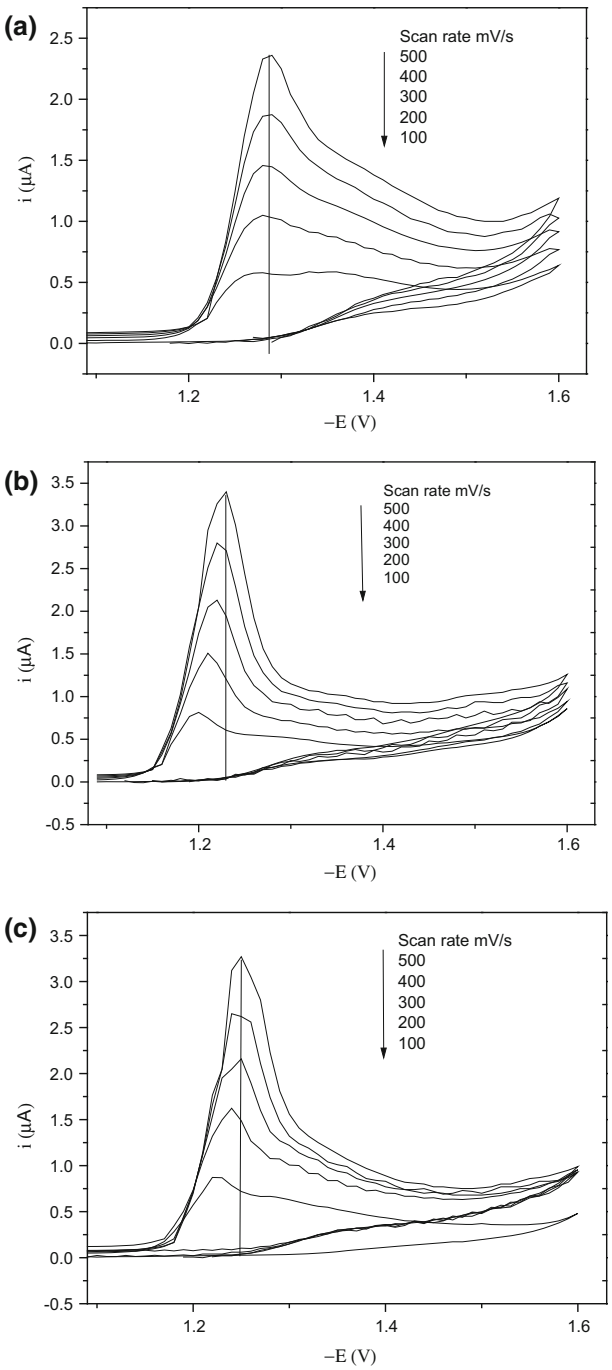

Fig. 3 Cyclic voltammograms of **a** STBT, **b** BTN_1, and **c** BTN_2 in pH = 7 and **c** pH = 10 at different scan rates of 100, 200, 300, 400 and 500 $mV{\cdot}s^{-1}$

fluorescence maxima (λ_{max}^{F}) of STBT, BTN_1 and BTN_2 in the different solvents, while Fig. 6 shows the normalized electronic absorption and fluorescence spectra of STBT, BTN_1 and BTN_2 in different solvents, as representative examples. The absorption spectra

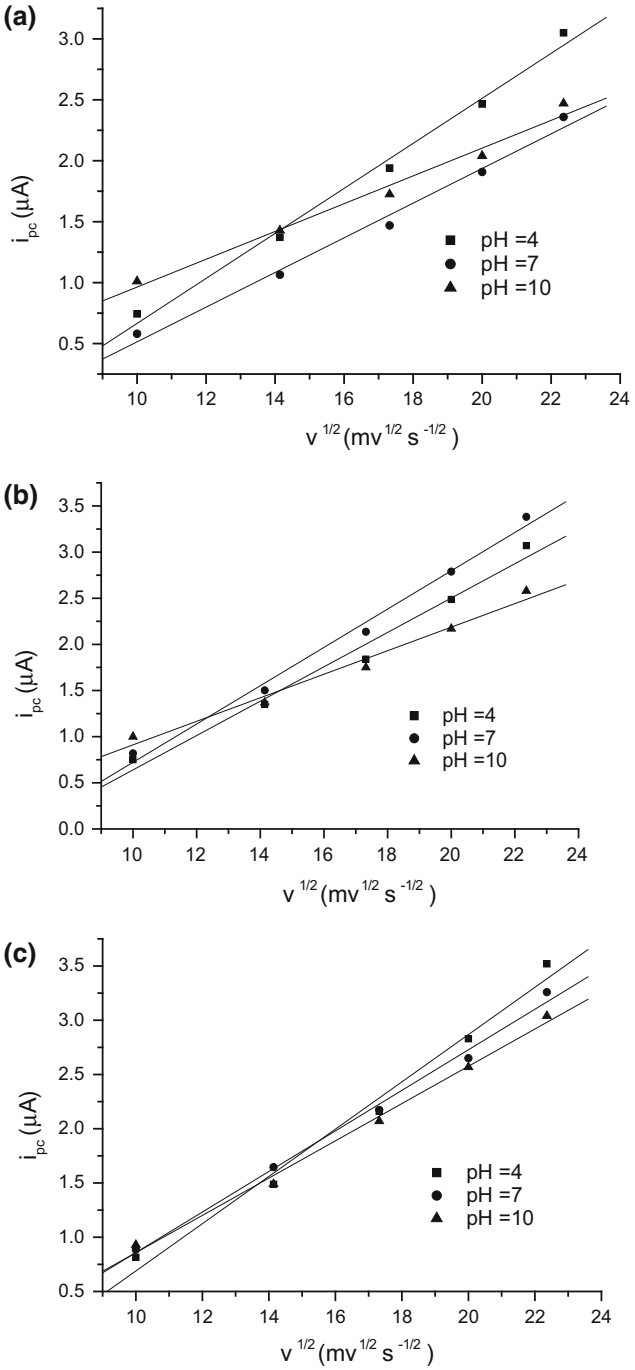

Fig. 4 Dependence of the cathodic peak current (i_{pc}) on the square root of the scan rate for the investigated compounds at different pH values

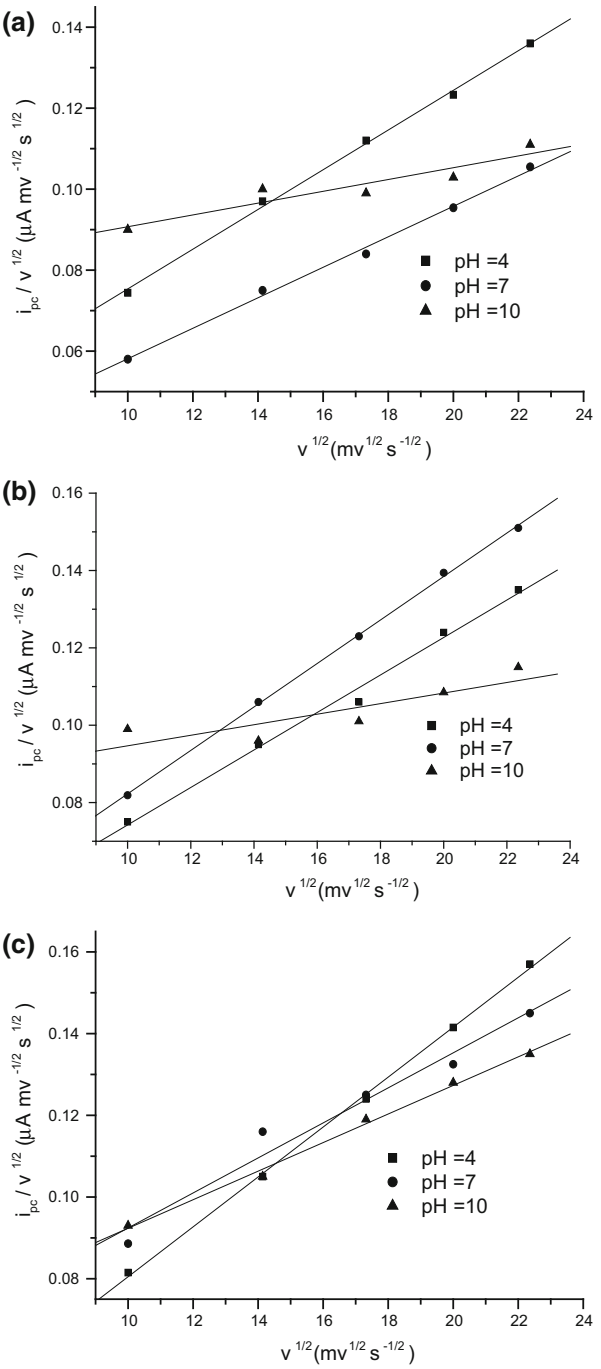

Fig. 5 Dependence of the current function ($i_{pc}/v^{1/2}$) on the square root of scan rates for the investigated compounds at different pH values

show maxima between 330 and 363 nm while the fluorescence spectra show maxima in the range 393–443 nm, with a shift depending on the solvent and the ring size. Generally, the absorption spectra show small solvent dependence. The shifts of the absorption band

Table 1 Cyclic voltammetric data for the reduction of STBT, BTN_1 and BTN_2 in pH = 4 as a function of the potential scan rate

Scan rate ($mV{\cdot}s^{-1}$)	STBT			BTN_1			BTN_2		
	i_{pc} (μA)	$-E_{pc}$ (V)	$i_{pc}/\nu^{1/2}$ ($\mu A{\cdot}mV^{1/2}.s^{-1/2}$)	i_{pc} (μA)	$-E_{pc}$ (V)	$i_{pc}/\nu^{1/2}$ ($\mu A{\cdot}mV^{1/2}.s^{-1/2}$)	i_{pc} (μA)	$-E_{pc}$ (V)	$i_{pc}/\nu^{1/2}$ ($\mu A{\cdot}mV^{1/2}.s^{-1/2}$)
100	0.74	1.02	0.074	0.8	0.96	0.08	0.82	0.97	0.02
200	1.37	1.03	0.1	1.35	0.97	0.1	1.48	0.98	0.11
300	1.94	1.03	0.112	1.84	0.98	0.11	2.16	0.99	0.124
400	2.46	1.04	0.123	2.48	0.98	0.124	2.83	0.99	0.14
500	3.05	1.041	0.14	3.02	0.98	0.14	3.52	1.0	0.16

Table 2 Cyclic voltammetric data for the reduction of STBT, BTN_1 and BTN_2 in pH = 7 as a function of the potential scan rate

Scan rate ($mV{\cdot}s^{-1}$)	STBT			BTN_1			BTN_2		
	i_{pc} (μA)	$-E_{pc}$ (V)	$i_{pc}/\nu^{1/2}$ ($\mu A{\cdot}mV^{1/2}.s^{-1/2}$)	i_{pc} (μA)	$-E_{pc}$ (V)	$i_{pc}/\nu^{1/2}$ ($\mu A{\cdot}mV^{1/2}.s^{-1/2}$)	i_{pc} (μA)	$-E_{pc}$ (V)	$i_{pc}/\nu^{1/2}$ ($\mu A{\cdot}mV^{1/2}.s^{-1/2}$)
100	0.58	1.27	0.058	0.82	1.198	0.082	0.886	1.227	0.09
200	1.065	1.278	0.08	1.5	1.209	0.11	1.646	1.24	0.12
300	1.469	1.28	0.08	2.14	1.21	0.123	2.17	1.251	0.13
400	1.908	1.28	0.1	2.79	1.22	0.14	2.65	1.24	0.133
500	2.359	1.29	0.11	3.38	1.23	0.15	3.26	1.25	0.15

Table 3 Cyclic voltammetric data for the reduction of STBT, BTN_1 and BTN_2 in pH = 10 as a function of the potential scan rate

Scan rate ($mV{\cdot}s^{-1}$)	STBT			BTN_1			BTN_2		
	i_{pc} (μA)	$-E_{pc}$ (V)	$i_{pc}/\nu^{1/2}$ ($\mu A{\cdot}mV^{1/2}.s^{-1/2}$)	i_{pc} (μA)	$-E_{pc}$ (V)	$i_{pc}/\nu^{1/2}$ ($\mu A{\cdot}mV^{1/2}.s^{-1/2}$)	i_{pc} (μA)	$-E_{pc}$ (V)	$i_{pc}/\nu^{1/2}$ ($\mu A{\cdot}mV^{1/2}.s^{-1/2}$)
100	0.99	1.59	0.099	1.0	1.484	0.099	0.93	1.503	0.093
200	1.425	1.602	0.100	1.37	1.486	0.096	1.49	1.506	0.11
300	1.722	1.607	0.99	1.75	1.4869	0.101	2.07	1.516	0.12
400	2.058	1.604	0.103	2.17	1.489	0.11	2.568	1.52	0.13
500	2.49	1.602	0.111	2.58	1.49	0.12	3.04	1.522	0.14

maximum λ^{A}_{max} are 2, 5 and 6 nm for BTN_2, STBT and BTN_1, while the fluorescence band maxima shifts by about 10, 12 and 15 nm for STBT, BTN_1 and BTN_2, respectively, with changing the solvent from EtOH to cyclohexane.

The fluorescence of STBT, BTN_1 and BTN_2 were effectively quenched by some aliphatic (TEA and DABCO) and aromatic amines (DMA and aniline) in the polar solvents EtOH, MeOH and ACN and non-polar cyclohexane at room temperature (Fig. 7). In fact,

Table 4 The absorption and emission maxima of STBT, BTN_1 and BTN_2 in different solvents

Compound	STBT		BTN_1		BTN_2	
Solvent	λ^{a}_{max} (nm)	λ^{f}_{max} (nm)	λ^{a}_{max} (nm)	λ^{f}_{max} (nm)	λ^{a}_{max} (nm)	λ^{f}_{max} (nm)
ACN	331	399	353	435	350	413
MeOH	333	403	358	437	350	418
EtOH	335	403	357	436	352	417
Cyclohexane	330	393	351	424	350	402

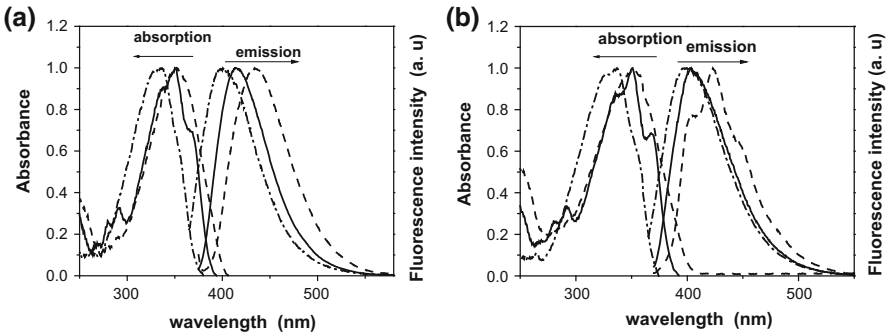

Fig. 6 Normalized absorption and emission spectra of (*dotted lines*) STBT, (*dashed line*) BTN_1 and (*solid line*) BTN_2 in **a** ACN and **b** cyclohexane

the absorption spectra of the fluorophore do not show any changes on addition of amines, which indicates the absence of ground state complex formation. Also, there was no change in the shape and position of the fluorescence spectra, even with higher concentrations of the quencher in the solvents, except for cyclohexane. This confirms the absence of any diarylethylenes–amine excited state complex (exciplex) formation. However, for STBT, BTN_1 and BTN_2–DMA pairs in non polar solvents, a new structureless red shifted emission band (corresponding to formation of an exciplex) is observed at sufficiently high concentrations of DMA (0.5–0.65 mol·dm^{-3}), where the fluorescence is almost completely quenched and the exciplex emission is symmetrically increased around this band. Similar observations were reported for trans-stilbene, disubstituted anthraquinones and substituted styrylthiophene [15–17].

Quenching of steady state fluorescence intensity of the investigated compounds by the used amines was analyzed using the Stern–Volmer (SV) relationship as:

$$\frac{I_0}{I} = 1 + K_{SV}[Q] \tag{1}$$

$$K_{SV} = k_q \tau_f \tag{2}$$

where I_o and I are the fluorescence intensities in the absence and presence of quencher, K_{SV} is the Stern–Volmer rate parameter constant, k_q is the bimolecular quenching rate constant, [Q] is the quencher concentration and τ_f is the fluorescence lifetime of diarylethylenes. Representative Stern–Volmer plots are shown in Fig. 8. It can be observed that the plots are linear for STBT, BTN_1 and BTN_2/DMA and/TEA pairs in EtOH, MeOH and cyclohexane, as examples, with different quencher concentrations in the range

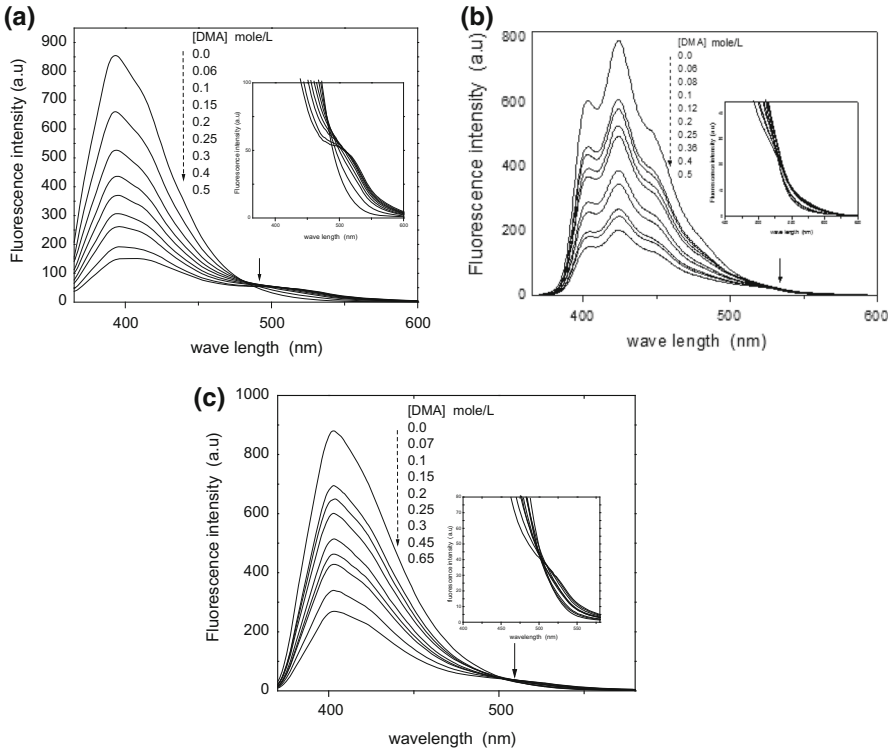

Fig. 7 The fluorescence spectra of **a** STBT, **b** BTN1 and **c** BTN2 with DMA in cyclohexane

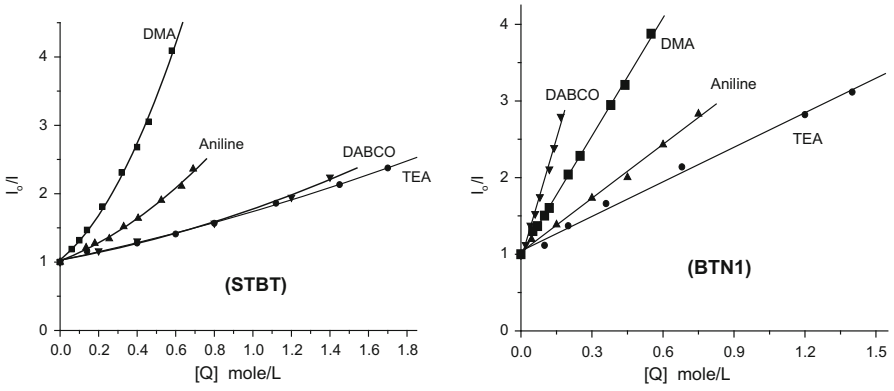

Fig. 8 Stern–Volmer plots for the fluorescence quenching of STBT and BTN1 using different amines as quenchers in ACN and cyclohexane, respectively

0.02–1.6 mol·dm^{-3}. However, they show an upward curvature at higher quencher concentrations, as in case of STBT, BTN_1 and BTN_2/DMA pairs in ACN. Similar experimental results were also observed for 3-carboxy-5,6-benzocoumarin, 1,4-bis[2-(2-methylphenyl)ethenyl]-benzene and 5,6-benzoquinoline [18–20]. In such cases, the values of K_{SV} were calculated from the linear parts of the plots, which indicate a dynamic process

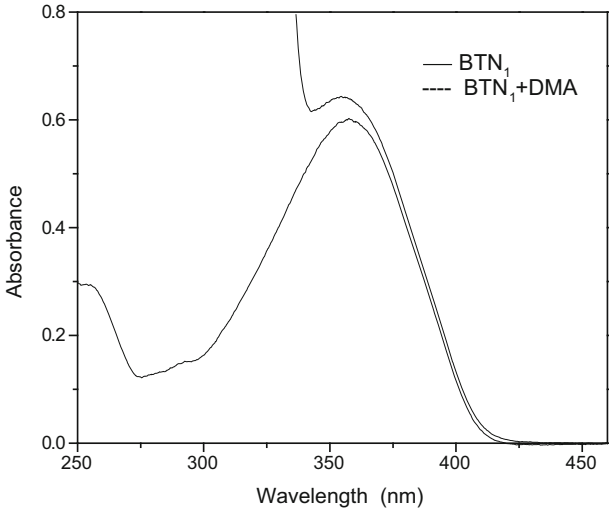

Fig. 9 The absorption spectra of BTN_1 with DMA in MeOH

in which quenching is mainly due to collision. The upward curvature suggests that the quenching mechanism is not purely diffusion controlled and may be associated with either ground state complex formation or to a transient, where the amine can quench the fluorescence of the diarylethylenes without collision (presence of a quenching sphere). To see whether the ground state complex formation is partly involved, the extended Stern–Volmer equation [21, 22] was tested:

$$\frac{(I_0/I)-1}{[\mathrm{Q}]} = \left(K_{\mathrm{SV}} + K_{\mathrm{g}}\right) + K_{\mathrm{SV}}K_{\mathrm{g}}[\mathrm{Q}] \tag{3}$$

where K_{SV} is the Stern–Volmer constant and K_g is the ground state association constant. From Eq. 3, the values of K_{SV} and K_g can be easily determined by least-squares fit of the relation between $[(I_o/I)-1]/[Q]$ and [Q]; the values of K_{SV} according to Eq. 3 were found to be imaginary in all the solvents. Therefore, the role of ground state complex formation is ruled out in the present cases, which is also confirmed by the absorption spectral measurements (Fig. 9). These finding show that Eq. 3 is not applicable to the data responsible for the observed positive deviation in the Stern–Volmer plots. Thus, analysis of this deviation was made using the quenching sphere static model. The Stern–Volmer constants were determined from the slopes of the corresponding plots and summarized in Tables 5, 6, 7, and 8.

To calculate the bimolecular quenching rate constant (k_q), the value of the fluorescence lifetime should be known. Unfortunately this technique was unavailable and its value was measured for BTN_1 and BTN_2 in a few solvents using a frequency modulation technique. The values in the remaining solvents as well as for STBT in all solvents were theoretically calculated. In this aspect, the fluorescence quantum yield (Φ_f) was firstly determined in all used solvents. The fluorescence quantum yield was determined relative to quinine sulphate in 0.05 $mol{\cdot}dm^{-3}$ H_2SO_4 ($\Phi_f = 0.54$) [23], using solutions having absorbance less than 0.3 at the excitation wavelength. The Φ_f values were calculated according to the following equation:

Table 5 Stern–Volmer constants for STBT, BTN_1 and BTN_2 with different quenchers in MeOH

Quencher	K_{SV} ($mol^{-1}\cdot dm^3$)	$k_q \times 10^9$ ($mol^{-1}\cdot dm^3\cdot s^{-1}$)	$[Q]_{1/2}$ ($mol^{1/2}\cdot dm^{-3/2}$)	Φ_f	τ (ns)
STBT				0.015	0.108
DMA	2.8	26.01	0.24		
TEA	0.32	2.96	–		
Amiline	1.4	12.95	0.66		
DABCO	0.66	6.1	1.42		
BTN_1				0.02	0.093
DMA	2.3	24.5	0.42		
TEA	0.1	1.03	–		
Amiline	1.3	13.4	0.8		
DABCO	0.19	2.03	0.4		
BTN_2				0.047	0.047
DMA	3.35	71.2	0.16		
TEA	0.34	7.32	–		
Amiline	1.72	36.5	0.54		
DABCO	0.72	15.3	1.4		

Table 6 Stern–Volmer constants for STBT, BTN_1 and BTN_2 with different quenchers in EtOH

Quencher	K_{SV} ($mol^{-1}\cdot dm^3$)	$k_q \times 10^9$ ($mol^{-1}\cdot dm^3\cdot s^{-1}$)	$[Q]_{1/2}$ ($mol^{1/2}\cdot dm^{-3/2}$)	Φ_f	τ (ns)
STBT				0.019	0.133
DMA	3.11	23.4	0.2		
TEA	0.34	2.5	–		
Amiline	1.7	12.4	0.64		
DABCO	0.76	5.7	1.07		
BTN_1					
DMA	2.9	30.1	0.26	0.027	0.096
TEA	0.14	1.5	–		
Amiline	1.5	15.2	0.7		
DABCO	0.6	6.3	1.4		
BTN_2				0.049	0.052
DMA	3.8	72.6	0.22		
TEA	0.38	7.4	–		
Amiline	1.8	35.4	0.54		
DABCO	0.9	16.9	0.9		

$$\Phi_f^u = \Phi_f^s \frac{n_u^2}{n_s^2} \frac{A^s}{A^u} \frac{\int I_f^u(\lambda_f)d\lambda_f}{\int I_f^s(\lambda_f)d\lambda_f} \quad (4)$$

where n is the refractive index of the solvent, A is the absorbance, Φ_f is the quantum yield, and the integrals denote the computed area under the corrected fluorescence bands. The subscripts s and u refer to the standard and test sample, respectively. Tables 5, 6, 7, and 8, show the fluorescence quantum yield of the investigated diarylethylenes in different solvents at room temperature.

Table 7 Stern–Volmer constants for STBT, BTN_1 and BTN_2 with different quenchers in ACN

Quencher	K_{SV} ($mol^{-1}\cdot dm^3$)	$k_q \times 10^9$ ($mol^{-1}\cdot dm^3\cdot s^{-1}$)	$[Q]_{1/2}$ ($mol^{1/2}\cdot dm^{-3/2}$)	Φ_f	τ (ns)
STBT				0.024	0.19
DMA	0.58	30.4	0.25		
TEA	2.41	12.7	0.46		
Amiline	3.2	16.6	0.35		
DABCO	1.7	8.8	0.33		
BTN_1				0.045	0.114
DMA	4.1	35.8	0.19		
TEA	1.99	17.5	0.62		
Amiline	2.6	22.5	0.46		
DABCO	1.1	9.3	0.92		
BTN_2				0.011	0.065
DMA	6.1	93.6	0.24		
TEA	2.50	38.4	0.70		
Amiline	4.1	62.4	0.33		
DABCO	2.01	30.8	0.51		

Table 8 Stern–Volmer constants for STBT, BTN_1 and BTN2 with different quenchers in cyclohexane

Quencher	K_{SV} ($mol^{-1}\cdot dm^3$)	$k_q \times 10^9$ ($mol^{-1}\cdot dm^3\cdot s^{-1}$)	$[Q]_{1/2}$ ($mol^{1/2}\cdot dm^{-3/2}$)	Φ_f	τ (ns)
STBT				0.14	0.392
DMA	6.9	17.7	0.12		
TEA	2.9	7.3	0.37		
Amiline	5.95	15.1	0.16		
DABCO	6.6	16.7	0.12		
BTN_1				0.34	0.38
DMA	4.99	13.13	0.23		
TEA	3.6	9.5	0.4		
Amiline	4.6	11.97	0.24		
DABCO	6.53	17.2	0.10		
BTN_2				0.44	0.23
DMA	8.1	35.2	0.15		
TEA	4.4	19.04	0.3		
Amiline	6.8	29.5	0.23		
DABCO	8.74	38.0	0.1		

The radiative rate constants were determined using the following equation:

$$k_R = 0.67\bar{\nu}_f^2 f \tag{5}$$

where $\bar{\nu}_f^2$ is the frequency of the emission maximum (cm^{-1}) and f is the oscillator strength, which was calculated as:

Table 9 Fluorescence lifetime (τ_f, ns) of diarylethylenes in various solvents calculated experimentally and theoretically

Compound	Experimental τ_f		Calculated τ_f		
	BTN_1	BTN_2	BTN_1	BTN_2	STBT
EtOH	0.9	0.05	0.096	0.052	0.133
MeOH	–	–	0.093	0.047	0.108
ACN	0.11	0.06	0.114	0.065	0.19
Cyclohexane	0.34	0.21	0.38	0.23	0.392

$$f = 4.32 \times 10^{-9} \varepsilon_{max} \Delta\bar{\nu}_{1/2} \tag{6}$$

where $\Delta\bar{\nu}_{1/2}$ is the wave number at the half band width of the absorption band.

Finally, the fluorescence lifetime (τ_f) was calculated by:

$$\tau_f = \frac{\Phi_f}{k_R} \tag{7}$$

The values of fluorescence lifetime calculated theoretically and the experimental ones for the investigated compounds in different solvents are summarized in Table 9. To test the precision of the calculated values, they were compared with the experimental ones. Therefore, the calculated τ_f values could be used safely for calculation of the bimolecular quenching constants. The calculated bimolecular rate constants are summarized in Tables 5, 6, 7, and 8. From the data, it was found that the k_q values for diarylethyles–DMA, –TEA and –aniline systems in ACN are higher than those in cyclohexane, suggesting the greater charge transfer character of the excited complex in ACN. Also, polar solvents like ACN enhance the dissociation of the formed ion pairs into solvent separated ones, which reduces the possibility of back electron transfer. In contrast, the behavior in the case of diarylethylenes–DABCO pairs is different, where the values of k_q in ACN are smaller than those in cyclohexane, which may be due to chemical nature of DABCO. For example, k_q values for STBT, BTN_1 and BTN_2–DMA pairs are 30.4, 35.8 and 93.6 $\times$ 10^9 $mol^{-1}{\cdot}dm^3{\cdot}s^{-1}$ in ACN, while in cyclohexane, the values are 17.7, 13.13 and 35.2 $\times$ 10^9 $mol^{-1}{\cdot}dm^3{\cdot}s^{-1}$, respectively. But for STBT, BTN_1 and BTN_2–DABCO pairs, the k_q values in ACN are 8.8, 9.3 and 30.8 $\times$ 10^9 $mol^{-1}{\cdot}dm^3{\cdot}s^{-1}$ while in cyclohexane, the values are 16.7, 17.2 and 38.0 $\times$ 10^9 $mol^{-1}{\cdot}dm^3{\cdot}s^{-1}$. As can be seen, the values of k_q for all if the amines in MeOH and EtOH are smaller than those in ACN. This is due to the hydrogen-bond donating ability of alcohols, which suppress the electron transfer process from the hydrogen bonded amines to the diarylethylenes [24]. For example, the values of k_q of STBT, BTN_1 and BTN_2–TEA pairs in MeOH are 2.96, 1.03 and 7.23 $\times$ 10^9 $mol^{-1}{\cdot}dm^3{\cdot}s^{-1}$ while in ACN, the values are 12.7, 17.5 and 38.4 $\times$ 10^9 $mol^{-1}{\cdot}dm^3{\cdot}s^{-1}$, respectively. Additionally, no general trend was observed for the effect of solvent polarity for quenching of the investigated diarylethylenes using amines which may be due to the antagonistic effect of other factors such as hydrogen-bonding character and viscosity of solvents, which affect the quenching efficiency. Also, aliphatic amines like TEA and DABCO are less efficient quenchers than aromatic amines such as DMA and aniline. This is in agreement with that reported by Inada et al. [25], who found that N-donors are less efficient than π-ones by 0.5 eV. Also, the calculated half quencher concentrations $[Q]_{1/2}$ (which is the quencher concentration at which $I_f = 1/2\ I_o$) confirm this finding; thus on using aliphatic amines, especially TEA, the $[Q]_{1/2}$ values are very large compared to those of the aromatic amines. As example, the $[Q]_{1/2}$ values of BTN_2–DMA, –aniline, –DABCO

Table 10 Energy of singlet–singlet transition, E^{D}_{00}, oxidation potentials, E^{D}_{exid}, and basicity (pK_b) of the amines

Parameter	Aromatic amines		Aliphatic amines	
	Aniline	DMA	TEA	DABCO
E^{D}_{00} (eV)[a]	3.91	3.81	>4.95	>4.35
E^{D}_{exid} (V)	0.93	0.78	1.05	0.70
pK_b	9.37	5.1	3.19	5.3

[a] 1 eV corresponds to 96.5 kJ·mol^{-1}

and –TEA, pairs are 0.24, 0.33, 0.51 and 0.7 mol·dm^{-3}, respectively, in ACN and in cyclohexane the corresponding values are 0.15, 0.23 and 0.1 and 0.3 mol·dm^{-3}, respectively.

A cursory glance at data reported in Table 10, shows that the k_q values for different diarylethylenes–amine pairs do not correlate with the basicity (pK_b) of the amines [26]. Accordingly, the k_q values for aliphatic amines are always lower than those of the aromatic amines, though it was expected to be opposite on the basis of their pK_b values. Similarly, among different aliphatic amines, although their pK_b values are quite similar, they have very different k_q values that cannot be justified on the basis of the difference in basicity of the aliphatic amines.

Considering the quenching mechanism, although some alternatives can be considered, based on the results, the ET from ground state amines to the excited fluorescent diarylethylenes seems to be the most likely mechanism, as suggested in earlier literature [27]. For the present systems, E^{D}_{100} values of the amines are much higher than those of the investigated diarylethylenes; E^{D}_{100} (the energy of the singlet–singlet transition was calculated from the intersection between the normalized absorption and emission spectra Table 11), which rules out the energy transfer as a quenching mechanism. Also, the bimolecular quenching constant for the different diarylethylenes–amine systems gradually decreases with increasing oxidation potentials (E^{D}_{exid}) of the amines. Figure 10 shows the correlation between k_q and E^{D}_{exid} for diarylethylenes–amine pairs in cyclohexane, as an example. As can be seen, BTN_2 is more sensitive to the change in the oxidation potential of the used amine compared to BTN_1 and STBT.

Since, the rate of ET reaction depends on the change in Gibbs energy, therefore, to give a quantitative description of ET process as the mechanism, it was necessary to estimate the change in the standard state Gibbs energy (ΔG°) for each diaryletylene–amine system in ACN and cyclohexane, as examples. The usual expression for calculation of ΔG° is Rehm–Weller equation [28], as follows:

Table 11 Energy of singlet–singlet transition, E^{A}_{00}, and reduction potentials, E^{A}_{red}, of the investigated compounds, measured in pH = 7 at scan rate = 500 mV·s^{-1}

Compound	STBT	BTN_1	BTN_2
E^{A}_{00} (eV)[a]	3.4	3.12	3.25
E^{A}_{red} (V)	1.29	1.23	1.25

[a] 1 eV corresponds to 96.5 kJ·mol^{-1}

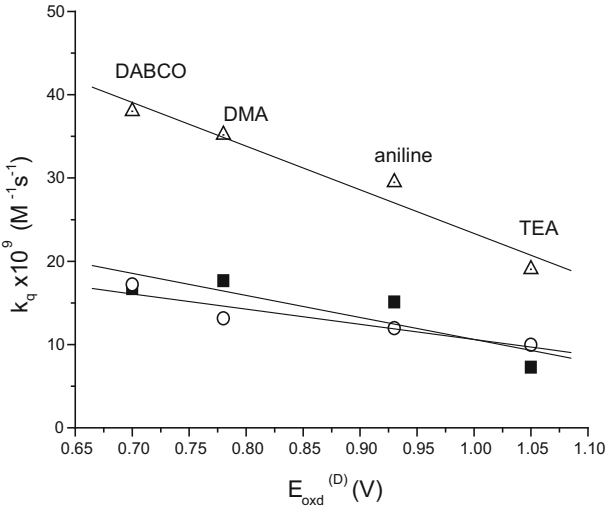

Fig. 10 The correlation of k_q versus E^D_{oxid} for STBT-(*filled square*), BTN_1-(*unfilled circle*) and (*unfilled triangle*) BTN_2–amine pairs in cyclohexane

$$\Delta G_o = E_{oxid} - E_{red} - E_{00} - \frac{e^2}{\varepsilon r} \tag{8}$$

where $e^2/\varepsilon r$ is the columbic attraction energy. E_{00} is the energy required for the transition of diaryethylenes from ground state (S_0) to first excited electronic state (S_1), which is obtained from the intersection points of normalized absorption and emission spectra. E^D_{exid} and E^A_{red} denote the oxidation potential of the donor and reduction potential of the acceptor, respectively. In the present case, the value of E^A_{red} was estimated using cyclic voltammetric measurements as discussed previously. The fourth term is negligible in highly polar solvents like ACN [29]. It is not possible to measure the redox potentials in cyclohexane; hence the Gibbs energy change ($\Delta G°$) in cyclohexane cannot be calculated using the previous equation. To obtain $\Delta G°$ in cyclohexane the corresponding values in ACN were shifted by a value of 0.698 eV (1 eV corresponds to 96.5 kJ·mol^{-1}) following the equation [30]:

$$\Delta G^{\circ}(\text{cyclohexane}) = \Delta G^{\circ}(\text{ACN}) + 0.698 \tag{9}$$

As seen from Table 12, the electron transfer reaction from the ground state amines to the excited diarylethylenes is highly exothermic and energetically favorable. Also, in all cases the rate constants are found to be the smallest for TEA, which is consistent with the low ($\Delta G°$) values. The most interesting observation is the inversion of the ET rate, Fig. 11, as predicted by Marcus outer sphere electron transfer theory [31], where the rate decreases in highly energetic systems. However, in cyclohexane the ET reaction rate falls in the normal and diffusion limit regions.

As mentioned previously, the fluorescence quenching of diarylethylenes in non-polar solvent such as cyclohexane is accompanied by the appearance of a new broad fluorescence band at longer wavelengths, which was attributed to exciplex formation (inset in Fig. 7). The exciplex emission spectra are associated with the quenching of STBT, BTN_1

Table 12 Gibbs energy changes and bimolecular rate constants of ET reactions in diarylethylenes–amine systems in ACN and cyclohexane

Compound	Quencher	ACN		Cyclohexane	
		$\Delta G°$ (kJ·mol^{-1})	$k_q \times 10^9$ (mol^{-1}·dm^3·s^{-1})	$\Delta G°$ (kJ·mol^{-1})	$k_q \times 10^9$ (mol^{-1}·dm^3·s^{-1})
STBT	TEA	−102	12.67	−35	7.27
	Aniline	−114	16.63	−46	15.1
	DMA	−128	30.36	−61	17.65
	DABCO	−136	8.78	−69	16.7
BTN_1	TEA	−81	17.45	−14	9.97
	Aniline	−93	22.5	−25	11.97
	DMA	−107	35.78	−40	13.13
	DABCO	−142	16.0	−74	17.2
BTN_2	TEA	−92	38.4	−24	19.04
	Aniline	−93	62.4	−36	29.47
	DMA	−107	93.6	−50	35.17
	DABCO	−140	30.84	−72	38.0

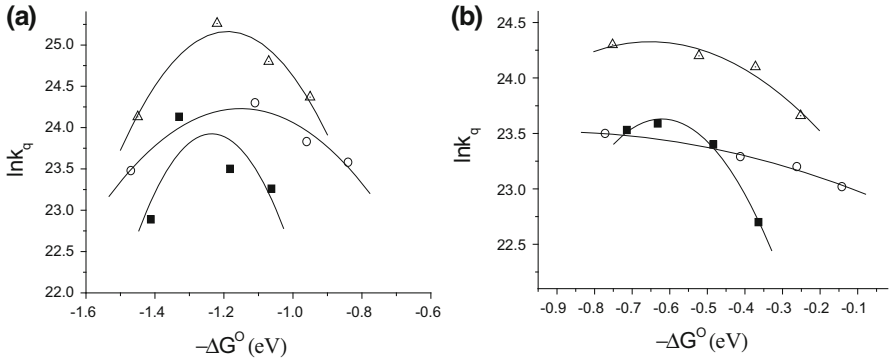

Fig. 11 Variation of ln k_q verus $\Delta G°$ for STBT-(*filled square*), BTN_1-(*unfilled circle*) and (*unfilled triangle*) BTN_2–amines pairs in **a** ACN and **b** cyclohexane

and BTN_2–DMA pairs in non-polar solvent, cyclohexane. The observed energies at the exciplex fluorescence maxima (E_1) are listed in Table 13 and can be compared with the theoretical energies E_2 according to Rehm and Weller:

$$E_2 = E_{\text{oxd}}^{(\text{D})} - E_{\text{red}}^{(\text{A})} - 0.15 \pm 0.1 \text{ eV} \quad (10)$$

For most stable exciplexes the correlation between E_1 and E_2 is better. The effect of structure on the stability of the exciplexes can be seen from the calculation of the exciplex dissociation enthalpies (E_3) [32]:

Table 13 Comparison of the observed energy at exciplex emission maxima, E_1, with the theoretical energy according to Rehm and Weller, E_2 and dissociation enthalpies, E_3, of the diarylethylenes–DMA exciplexes in cyclohexane

STBT				BTN_1				BTN_2			
λ (nm)	E_1 (eV)[a]	E_2 (eV)	E_3 (eV)	λ (nm)	E_1 (eV)[a]	E_2 (eV)	E_3 (eV)	λ (nm)	E_1 (eV)[a]	E_2 (eV)	E_3 (eV)
491	2.52	1.92	3.7	534	2.1	1.86	3.4	507	2.44	1.88	3.59

[a] 1 eV corresponds to 96.5 kJ·mol^{-1}

$$E_3 = E_{00} - E^{D}_{oxid} - E^{A}_{red} - 0.13 \text{ ev} \quad (11)$$

where E_{oo} is the singlet excitation energy of diaryletylenes. The higher exciplex dissociation enthalpies, Table 13, indicate strongly bound exciplexes.

In the line of the above results, it can be concluded that the fluorescence quenching of 1,2-diarylethylenes by aliphatic and aromatic amines is due to the electron transfer (ET) from the ground state amines to the excited diarylethylenes. Aliphatic amines like TEA and DABCO are less efficient quenchers than aromatic amines such as DMA and aniline. The hydrogen-bond donating ability of protic solvents like MeOH or EtOH plays an important role in the quenching process, leading to an observable decrease in quenching efficiency (k_q) compared to an aprotic solvent like ACN. The observed k_q values for different diarylethylenes–amine pairs do not correlate with the basicity (pK_b) of the amines but decrease with increasing the oxidation potentials of the amines. The ET reaction from the ground state amines to excited state diarylethylenes is highly exothermic and energetically favorable, and k_q values have been correlated with ΔG° values for the ET reactions from Marcus outer-sphere ET theory.

References

1. Pang, S., Hyun, H., Lee, S., Jang, D., Lee, M.J., Kang, S.H., Ahn, K.-H.: Photoswitchable fluorescent diarylethene in a turn-on mode for live cell imaging. Chem. Commun. **48**, 3745–3747 (2012)
2. Sabbioni, E., Blanch, N., Baricevic, K., Sera, M.A.: Effects of trace metal compounds on HIV-1 reverse transcriptase. Biol. Trace Etem. Res. **68**, 107–119 (1999)
3. Krieg, R., Halbhuber, K.J.: Novel oxidative self-anchoring fluorescent substrates for the histochemical localization of endogenous and immunobound peroxidase activity. J. Mol. Histol. **35**, 471–487 (2004)
4. Tanifuji, N., Irie, M., Matsuda, K.: Photoswitching of solvatochromism using diarylethenes with 2,5-disubstituted 3-thienyl unit. Chem. Lett. **36**, 1232–1233 (2007)
5. Zhao, M., Samoc, M., Prasad, P.N., Reinhardt, B.A., Unroe, M.R., Prazak, M., Evers, R.C., Kane, J.J., Jariwala, C., Sinsky, M.: Studies of third-order nonlinearities of model compounds containing benzothiazole, bensimidazole and benzoxazole units. Chem. Mater. **2**, 670–678 (1990)
6. Jeong, Y.C., Ik Yang, S., Ahn, K.-H., Kim, E.: Highly fluorescent photochromic diarylethene in the closed-ring form. Chem. Commun. **19**, 2503–2505 (2005)
7. Marcus, R.A., Sutin, N.: Electron transfers in chemistry and biology. Biochem. Biophys. Acta. **811**, 265–322 (1985)
8. Yoshihara, K., Tominaga, K., Nagasawa, Y.: Effects of the solvent dynamics and vibrational motions in electron transfer. Bull. Chem. Soc. Jpn **68**, 696–712 (1995)
9. Lewis, F.D., Dykstra, R.E.: Exciplex formation and behavior in the 9,10-dicyanoanthracene–stilbene system. J. Photochem. Photobiol., A **49**, 109–119 (1989)

10. Allonas, X., Jacques, P.: Factors affecting adiabaticity in bimolecular photoinduced electron-transfer reaction between anthracene-derivatives and organic donors. Chem. Phys. **215**, 371–378 (1997)
11. Nad, S., Pal, H.: Photo induced electron transfer from aliphatic amines to coumarin dyes. J. Chem. Phys. **116**, 1658–1670 (2002)
12. Satpati, A.K., Nath, S., Kumbhakar, M., Maity, D.K., Senthilkumar, S., Pal, H.: Bimolecular electron transfer reactions in coumarin–amine systems: donor–acceptor orientational effect on diffusion-controlled reaction rates. J. Mol. Struct. **878**, 84–94 (2008)
13. Vernigor, E.M., Shalaev, V.K., Novoseltesva, L.P., Lukyanets, E.A., Ustenko, A.A., Zvolinskii, V.P., Zakharov, V.F.: Khim. Geterotsikl. Soedin. **5**, 604 (1980)
14. Bard, A.J., Faulkner, L.R.: Electrochemical Methods-Fundamentals and Applicaions. Wiley, New York (1980)
15. Ho, T.I.: Structure reactivity relationship for fluorecence quenching of trans-stilbene by tertiary amines. J. Photochem. **36**, 185–192 (1987)
16. Hirendra, G.N., Haridas, P., Dipak, K.P., Tulsi, M., Jai, P.M.: Interaction of the excited singlet state of disubstituted anthraquinones with aliphatic and aromatic amines: a fluorescence quenching study. J. Photochem. Photobiol., A **73**, 17–22 (1993)
17. Chen, C.-C., Pan, K., Wang, S.-L., Ho, T.-I.: Styrylthio phene-amine exciplexes. J. Lumin. **71**, 321–328 (1997)
18. Tablet, C., Hilledrand, M.: Quenching of the fluorescence of 3-carboxy-5,6-benzocoumarin by aromatic amines. J. Photochem. Photobiol A: Chem. **189**, 73–79 (2007)
19. Thipperudrappa, J., Biradar, D.S., Hanagodimath, S.M.: Fluorescence quenching of 2,2″-dimethyl-*p*-terphenyl by carbon tetrachloride in different solvents and temperatures. J. Lumin. **126**, 339–346 (2007)
20. Carrigan, S., Doucette, S., Jones, C., Marzzacco, C.J., Halpern, A.M.: The fluorescence quenching of 5,6-benzoquinoline and its conjugate acid by Cl^-, Br^-, SCN^- and I^- ions. J. Photochem. Photobiol., A **99**, 29–35 (1996)
21. Behera, P.K., Mishra, A.K.: Static and dynamic model for 1-naphthol fluorescence quenching by carbon tetrachloride in dioxane–acetonitrile mixtures. J. Photochem. Photobiol., A **71**, 115–118 (1993)
22. Zeng, H., Durocher, G.: Analysis of fluorescence quenching in some antioxidants from nonlinear Stern–Volmer plots. J. Lumin. **63**, 75–84 (1995)
23. Maus, M., Rellig, W., Bonafoux, D., Lapouyade, R.: Photoinduced intramolecular charge transfer in a series of differently twisted donor–acceptor biphenyls as revealed by fluorescence. J. Phys. Chem. A **103**, 3388–3401 (1999)
24. Oh, S.-C., Shirota, Y., Mikawa, H., Kusabayashi, S.: The effect of the hydrogen bonding on the photoinduced electron transfer reaction of a naphthalene–triethylamine system in the presence of alcohols. Chem. Lett. **12**, 2121–2124 (1986)
25. Inada, T.N., Kikuchi, K., Takahashi, Y., Ikeda, H., Miyashi, T.: A comparative study on electron transfer by aliphatic and aromatic amines. J. Photochem. Photbiol. A **137**, 93–97 (2000)
26. Aggarwal, V.K., Emme, I., Fulford, S.Y.: Correlation between p*K*a and reactivity of quinuclidine-based catalysts in the Baylis–Hillman reaction—discovery of quinuclidine as optimum catalyst leading to substantial enhancement of scope. J. Org. Chem. **68**, 692–700 (2003)
27. Castner Jr, E.W., Kennedy, D., Cave, R.J.: Solvent as electron donor: donor/acceptor electronic coupling is a dynamical variable. J. Phys. Chem. A **104**, 2869–2885 (2000)
28. Rehm, D., Weller, A.: Bonding state and fluorescence spectra of hetero-excimer. Z. Phys. Chem. NF **69**, 183–200 (1970)
29. Weller, A.: Photoinduced electron transfer in solution: exciplex and radical ion pair formation free enthalpies and their solvent dependence. Z. Phys. Chem. NF **133**, 93–98 (1982)
30. Chen, J.M., Ho, T.-I., Mou, C.-Y.: experimental investigation of excited-state electron transfer reaction: effect of free energy and solvent on rates. J. Phys. Chem. **94**, 2889–2896 (1990)
31. Jortner, J., Bixon, M. (eds.): Electron Transfer from Isolated Molecules to Biomolecules (Adv. Chem. Phys. Part 1 and 2), vol. 106, 107. Wiley, New York (1999)
32. Knibbe, H., Rehm, D., Weller, A.: Thermodynamics of the formation of excited eda (electron donor–acceptor) complexes. Ber. Bunsen-Ges. Phys. Chem. **73**, 839–845 (1969)